Geophysical Research Letters

RESEARCH LETTER
10.1029/2020GL088363

Relative Importance of Greenhouse Gases, Sulfate, Organic Carbon, and Black Carbon Aerosol for South Asian Monsoon Rainfall Changes

Daniel M. Westervelt[1,2], Yujia You[1], Xiaoqiong Li[1], Mingfang Ting[1], Dong Eun Lee[1,3], and Yi Ming[4]

[1]Lamont-Doherty Earth Observatory of Columbia University, Palisades, NY, USA, [2]NASA Goddard Institute for Space Studies, New York, NY, USA, [3]Chungnam National University, Daejoeon, Daejoeon, South Korea, [4]NOAA Geophysical Fluid Dynamics Lab, Princeton, NJ, USA

Key Points:
- Per unit radiative forcing, black carbon is the most effective driver of precipitation change during the South Asian summer monsoon
- Anomalous sinking and rising explain modeled precipitation responses to anthropogenic greenhouse gases and aerosols
- The dynamic component dominates the mean column-integrated moisture flux convergence over the thermodynamic component

Supporting Information:
- Supporting Information S1

Correspondence to:
D. M. Westervelt,
danielmw@ldeo.columbia.edu

Citation:
Westervelt, D. M., You, Y., Li, X., Ting, M., Lee, D. E., & Ming, Y. (2020). Relative importance of greenhouse gases, sulfate, organic carbon, and black carbon aerosol for South Asian monsoon rainfall changes. *Geophysical Research Letters*, *47*, e2020GL088363. https://doi.org/10.1029/2020GL088363

Received 9 APR 2020
Accepted 3 JUN 2020
Accepted article online 15 JUN 2020

Abstract The contribution of individual aerosol species and greenhouse gases to precipitation changes during the South Asian summer monsoon is uncertain. Mechanisms driving responses to anthropogenic forcings need further characterization. We use an atmosphere-only climate model to simulate the fast response of the summer monsoon to different anthropogenic aerosol types and to anthropogenic greenhouse gases. Without normalization, sulfate is the largest driver of precipitation change between 1850 and 2000, followed by black carbon and greenhouse gases. Normalized by radiative forcing, the most effective driver is black carbon. The precipitation and moisture budget responses to combinations of aerosol species perturbed together scale as a linear superposition of their individual responses. We use both a circulation-based and moisture budget-based argument to identify mechanisms of aerosol and greenhouse gas induced changes to precipitation and find that in all cases the dynamic contribution is the dominant driver to precipitation change in the monsoon region.

Plain Language Summary Small particles suspended in the atmosphere and emitted by human activities, known as atmospheric aerosols, contribute to changes in precipitation in South Asia, yet the exact importance of individual components is not well understood. Further, the impact of human-caused greenhouse gas emissions is also uncertain. We use a computer model to simulate the monsoon and find that aerosols are the largest driver of precipitation change compared to greenhouse gases. We also breakdown the precipitation changes by their components and find that changes in atmospheric vertical and horizontal motion of air dominate over increases in moisture for explaining the total rainfall changes. These results help further understand the impact of climate change on precipitation in South Asia, which is important to the lives of billions of people.

1. Introduction

The South Asian summer monsoon is an integral component of life for billions of people, delivering 80% of annual mean precipitation for most regions of South Asia typically in the summer months of June–September (JJAS) (Webster et al., 1998). Numerous studies over the last two or more decades have sought to both explain the observed trends in precipitation in South Asia and to project how these patterns and trends may respond or have already responded to global change, with some studies pointing to a role for anthropogenic aerosols in the observed decreasing precipitation trends over the twentieth century (Bollasina et al., 2011; Gautam et al., 2009; Goswami et al., 2006; Guo et al., 2015; Lau & Kim, 2006, 2017; Li et al., 2015; Meehl et al., 2008; Menon et al., 2002; Turner & Annamalai, 2012). To date, however, there has been limited work focusing on the impact of individual atmospheric constituents, such as sulfate, black carbon (BC), and organic carbon (OC) aerosol, separately and together, on South Asian monsoon precipitation (Sanap & Pandithurai, 2015). We therefore seek to compare and contrast the individual impact of different anthropogenic aerosol species and greenhouse gases (GHG) on the South Asian summer monsoon.

Changes in anthropogenic aerosol and GHG emissions are important drivers of Earth's hydrologic cycle (Ramanathan et al., 2007; Rosenfeld et al., 2008). The net effect of historical increases in anthropogenic emissions between preindustrial and present-day has been linked to decreases in precipitation, especially in monsoon regions such as South Asia and West Africa (Biasutti & Giannini, 2006; Bollasina et al., 2011; Li et al., 2016; Undorf et al., 2018). While prior work has shown GHG and aerosols to have opposing effects

on monsoon precipitation (Lau & Kim, 2017; Li et al., 2015; Wang et al., 2016), it is expected that aerosols, as strong forcers in the shortwave, wield a larger influence than GHG (Liepert & Previdi, 2009; Liu et al., 2018; Samset et al., 2016; Wilcox et al., 2020). Forced changes to precipitation can be understood through changes in moisture and temperature (thermodynamic effects) or by changes in circulation (dynamic effects) (Bollasina et al., 2011; Marvel & Bonfils, 2013; Pfahl et al., 2017). In a coupled climate model with sea surface temperature (SST) feedbacks, surface warming of GHG increases the water vapor saturation pressure roughly exponentially as given by the Clausius-Clapeyron equation, thereby enhancing precipitation (Allen & Ingram, 2002; Held & Soden, 2006; Zhao et al., 2019) thermodynamically. The dynamic contribution from GHG and aerosols is much more uncertain, especially regionally (Li & Ting, 2017; Pfahl et al., 2017). Aerosol extinction of incoming solar radiation via direct and indirect effects results in weaker precipitation due to weakened circulation (Li et al., 2019; Ramanathan et al., 2001; Singh, 2016). Aerosol emissions and thus forcing are also spatially heterogeneous both zonally and meridionally, which can result in further enhancement of the circulation (dynamic) component of the precipitation response (Li et al., 2018; Shen & Zhao, 2020; Westervelt et al., 2017, 2018, 2020). Research has also shown that the fast response (using fixed SST) dominates the total aerosol-induced monsoon changes but that SST feedbacks are more important for the GHG-forced response (Li et al., 2018).

Formation of aerosol in the atmosphere is a result of emissions and multiphase chemical reactions including numerous inorganic and organic chemical species (Jimenez et al., 2009). Both aerosols local to South Asia and aerosols sourced from other world regions play an important role in South Asian monsoon precipitation (Westervelt et al., 2018). Aerosol composition in India is not well characterized especially outside of large cities; however, OC, sulfate, and BC are thought to be the largest contributors to overall aerosol submicron mass (Brooks et al., 2019; Gani et al., 2019; Schnell et al., 2018). Monsoon precipitation responses are dependent on aerosol composition. For example, BC and dust, absorbers of incoming shortwave radiation, are expected to have different impacts compared to sulfate aerosol, which is a scattering agent (Menon et al., 2002; Ming et al., 2010). Lau and Kim (2006) proposed an "elevated heat pump" hypothesis in which rising heat created from dust aerosol over the Tibetan Plateau (reinforced by local BC emissions) draws in warm and moist air from the southwest in the pre-monsoon season, enhancing monsoon rainfall. In addition to interaction with incoming solar radiation (aerosol direct effect), aerosols also impact precipitation indirectly by modulating cloud properties (aerosol indirect effect) (Penner et al., 2006). In particular, aerosol increase may increase the number and decrease the average size of cloud droplets (Twomey, 1977) theerby reducing the autoconversion rate, resulting in a suppression of precipitation (Albrecht, 1989), though this remains uncertain (Stevens & Feingold, 2009). One recent study has argued that climate response to aerosol may be dominated by these aerosol indirect effects (Chung & Soden, 2017). Additionally, Allen et al. (2019) find that semidirect effects of BC could exert a positive radiative forcing, which could have additional impacts on precipitation. Garrett and Zhao (2006) have investigated a cloud thermal emissivity effect that may trap longwave radiation and exert a warming influence on climate.

We expand on past work by conducting single-forcing experiments with an extensively used global climate model with detailed treatment of emissions and chemistry. A control simulation with preindustrial conditions is contrasted with simulations in which forcers such as BC, sulfate, OC, and well-mixed GHGs are individually set to year 2000 levels, with all other model features identical between the sets of simulations. All simulations use fixed SST fields such that the SST response (slow response) is not diagnosed in this paper. We also perturb different forcing agents together in order to understand the interplay between forcing agents and their additivity. We estimate the precipitation change by differencing perturbation simulations with the control and break down the precipitation response into dynamical and thermodynamical effects to better understand the underlying mechanisms. We also analyze changes in circulation in both horizontal and vertical directions. Finally, we compare the relative importance of each individual forcing agent on the South Asian summer monsoon.

2. Methods

2.1. Model and Simulations

We use the NOAA Geophysical Fluid Dynamics Atmospheric Model version 3 (GFDL-AM3), the atmospheric component of the fully coupled GFDL climate model (Donner et al., 2011). All simulations are

Table 1
List of Anthropogenic Emissions Perturbations Considered and Their Associated Global and Regional Effective Radiative Forcing

Case name	Response tested (all other forcings held consistent between simulations)	Global mean TOA radiative forcing in W m^{-2} (monsoon region mean)
GHG	2000 minus 1850 global anthropogenic greenhouse gases	2.57 (2.53)
SO4	2000 minus 1850 global anthropogenic sulfur emissions	−2.14 (−5.22)
BC	2000 minus 1850 global anthropogenic black carbon emissions	0.16 (0.86)
OC	2000 minus 1850 global anthropogenic organic aerosol emissions	−0.4 (−1.15)
SO4 + BC	2000 minus 1850 global anthropogenic sulfur and black carbon emissions	−1.94 (−4.21)
SO4 + BC + OC	2000 minus 1850 global anthropogenic sulfur, black carbon, and organic aerosol emissions	−1.57 (−4.41)

Note. Monsoon region is defined as 0–50 N latitude, 50–180°E longitude.

carried out with fixed 1950–2000 climatological SSTs in order to exclude any SST impacts. The model uses 48 vertical layers from the surface up to about 0.01 hPa and a six face cubed-sphere grid with 48 grid cells along each edge (C48), resulting in about a 200 km by 200 km horizontal resolution. Emissions of anthropogenic aerosols and their precursors are taken from Lamarque et al. (2010). Concentrations of long-lived GHG are specified according to Meinshausen et al. (2011). Aerosol activation into cloud droplets is parameterized according to Ming et al. (2006). Sulfate and BC are internally mixed with each other, whereas all other aerosols are externally mixed. Additional details on model description can be found in Donner et al. (2011) and Westervelt et al. (2017). Modeled JJAS precipitation rate compares well to Global Precipitation Climatology Project observed precipitation (Figure S1 in the supporting information), though the model underpredicts the highest precipitation rates. Further model evaluation for other fields in GFDL-AM3 can be found in Donner et al. (2011), Naik et al. (2013), and Westervelt et al. (2017).

We conducted a total of seven simulations, each 65 years long, using GFDL-AM3. The control simulation consisted of year 1850 anthropogenic pollutant emissions and GHG concentrations. We performed simulations changing aerosol emissions or GHG concentrations of a forcing agent to year 2000 levels globally while keeping all other conditions identical to the control, creating six perturbation cases as outlined in Table 1. For example, the "GHG" case refers to a difference between a simulation in which GHG concentrations are specified at year 2000 levels globally versus the control. Anthropogenic emissions of SO_2, BC, and OC are individually perturbed to 2000 levels and compared to the control to create three additional cases, and two additional cases consist of perturbing SO_2 and BC together and SO_2, BC, and OC together. All cases were differenced as 2000 emissions minus 1850, representing the impact of a large increase in the abundance of each forcing component (see Figure S2). We remove the first 5 years as spin-up and test for statistical significance using a Student's *t* test on seasonal mean responses with the null hypothesis being that the difference between the control and the perturbation simulation is zero.

2.2. Moisture Budget Calculation

To quantify physical mechanisms responsible for driving modeled precipitation changes, we employ a diagnostic atmospheric moisture budget analysis (Seager & Henderson, 2013; Seager et al., 2014). Briefly, the steady state moisture budget equation is as follows:

$$\overline{P}-\overline{E}=-\frac{1}{g\rho_w}\nabla\cdot\overline{\int_0^{p_s}\boldsymbol{u}qdp}\approx-\frac{1}{g\rho_w}\nabla\cdot\sum_{k=1}^{10}\overline{\boldsymbol{u_k}q_k\Delta p_k} \quad (1)$$

where precipitation (P) minus evaporation (E) is balanced by the moisture convergence (MC) term (right hand side), where ρ_w is density of water, g is acceleration due to gravity, p is atmospheric pressure, p_s is surface pressure, $\boldsymbol{u}$ is the horizontal wind vector, and q is specific humidity. Quantities are integrated over 10 total vertical levels k ranging from 1,000 to 200 hPa. The MC can be separated into a mean and transient eddy component. Previous work has found the transient eddy component to be negligible over the South Asian monsoon region (Li et al., 2018). We therefore quantify the forced response using the mean MC term as follows, with subscript F indicating the forced perturbation simulation (e.g., 2000 aerosol emissions) and C indicating the control simulation (e.g., 1850 emissions):

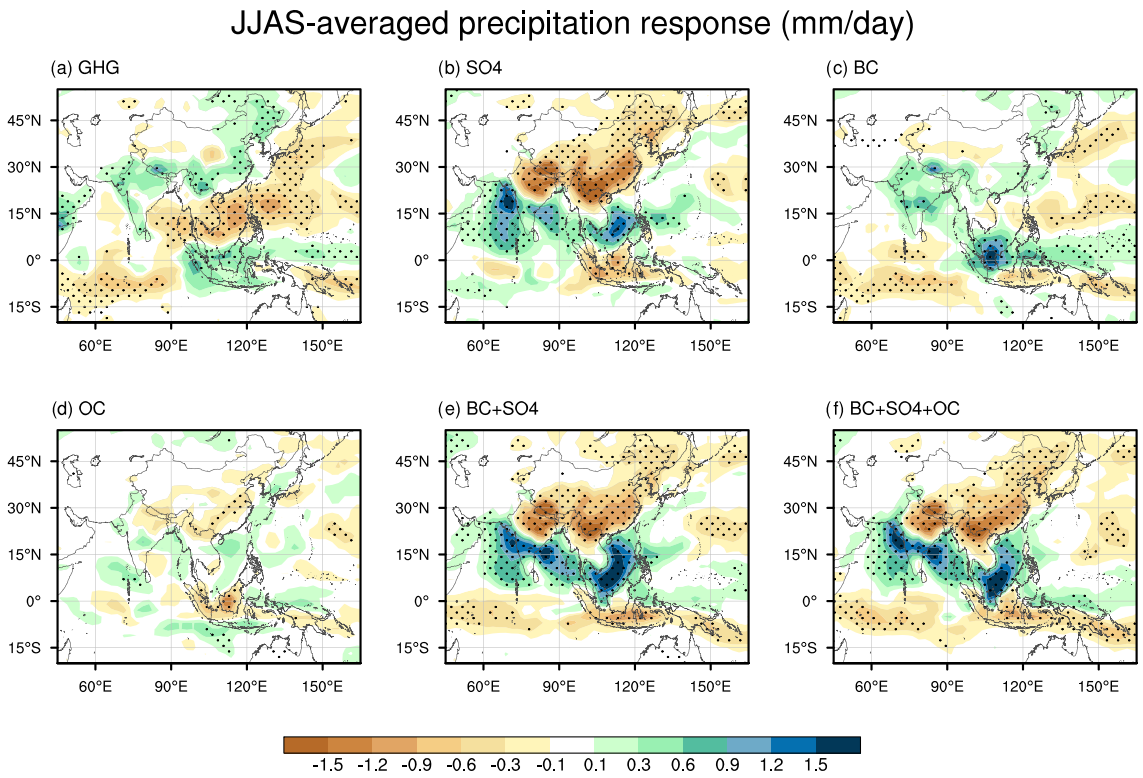

Figure 1. JJAS mean precipitation change in response to 2000 anthropogenic emissions compared to 1850 anthropogenic emissions for (a) greenhouse gases, (b) sulfate, (c) black carbon, (d) organic carbon aerosol, (e) black carbon and sulfate combined, and (f) black carbon, sulfate, and organic aerosol combined. Stippling indicates statistical significance at the 95% confidence interval using a Student's *t* test.

$$\Delta\overline{\overline{MC}} = \left(-\frac{1}{g\rho_w}\overline{\overline{\nabla\cdot\sum_{k=1}^{10}\boldsymbol{u_k}q_k\Delta p_k}}\right)_F - \left(-\frac{1}{g\rho_w}\overline{\overline{\nabla\cdot\sum_{k=1}^{10}\boldsymbol{u_k}q_k\Delta p_k}}\right)_C$$
$$\approx -\frac{1}{g\rho_w}\nabla\cdot\sum_{k=1}^{10}\overline{\overline{\boldsymbol{u}}}_{\boldsymbol{k},C}\Delta\overline{\overline{q}}_k\overline{\Delta p_k} - \frac{1}{g\rho_w}\nabla\cdot\sum_{k=1}^{10}\Delta\overline{\overline{\boldsymbol{u}}}_{\boldsymbol{k}}\overline{\overline{q}}_{k,C}\overline{\Delta p_k} \approx \Delta\overline{\overline{TH}} + \Delta\overline{\overline{DY}}$$

where double overbar refers to 60-year seasonal mean. The thermodynamic component (ΔTH), representing changes in moisture, and the dynamic component (ΔDY), representing changes in circulation approximately sum to the mean MC. For ΔTH, the circulation component is fixed via holding the wind vector, **u**, as the control simulation value. Conversely, the specific humidity (q) is held at control value to calculate ΔDY. The quadratic term representing covariances between **u** and q is found to be small compared to ΔDY and ΔTH and therefore has been neglected (Li et al., 2018).

3. Relative Importance of Anthropogenic Forcing Agents on Precipitation Response

The 60-year summertime precipitation response in each of our six cases (perturbation minus control simulation differences) is shown in Figure 1. As expected, increases in GHG (Figure 1a) increase precipitation over large swaths of land area in South and East Asia with some statistical significance, though over the ocean the opposite (drying) occurs. Increases in sulfate aerosols (Figure 1b) on the other hand significantly decrease precipitation over land areas in South and East Asia, especially over northern India, whereas additional wetting occurs over the surrounding ocean. Sulfate aerosols exert about a factor of 2 larger absolute change in precipitation rate compared to all well-mixed GHG combined. The precipitation response to BC is statistically significant wetting. Over India, precipitation rate increases by about 0.3 to 0.6 mm day^{-1} due to BC increases, partially offsetting some of the drying response caused by sulfate aerosol. Despite having a small total aerosol mass and a small aerosol radiative forcing (Table 1), BC has an outsized impact on monsoon

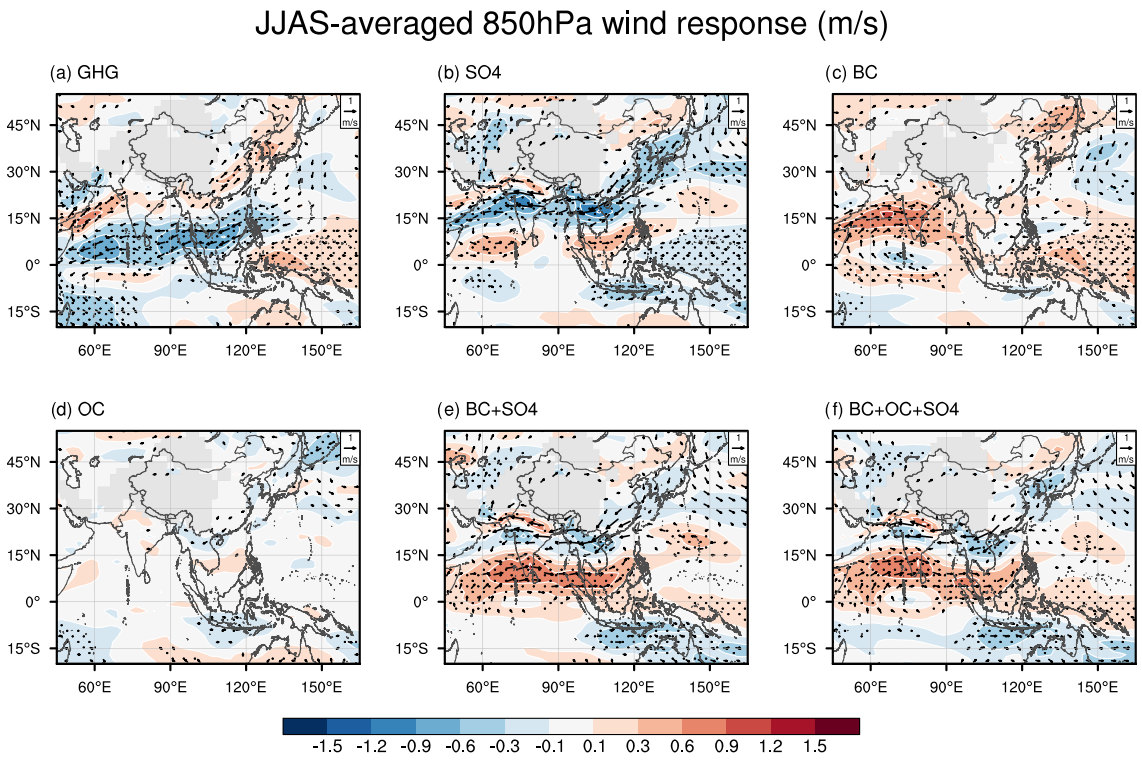

Figure 2. JJAS mean 850 hPa wind speed (shading) and direction (arrows) change in response to 2000 anthropogenic emissions compared to 1850 anthropogenic emissions for (a) greenhouse gases, (b) sulfate, (c) black carbon, (d) organic carbon aerosol, (e) black carbon and sulfate combined, and (f) black carbon, sulfate, and organic carbon aerosol combined.

precipitation. However, if all precipitation responses are normalized by either global radiative forcing (Figure S3) or monsoon region radiative forcing (Figure S4), BC is the most important driver of precipitation change during the JJAS monsoon season, followed by sulfate and GHG. Anthropogenic OC has a small and mostly insignificant effect on precipitation changes between 2000 and 1850, shown in Figure 1d. We attribute this to the lower hygroscopicity of OC compared to sulfate (Petters & Kreidenweis, 2007), hindering the direct forcing via scattering and the indirect forcing via cloud condensation nuclei formation. When BC and sulfate are perturbed together (Figure 1e), key features from each separate component are evident in the precipitation response, namely, a strong north–south dipole pattern with strong wetting from BC in South India and over the ocean and a slightly weaker drying over land due to the opposite competing effects from BC and sulfate. The dipole pattern seen here is robust across many atmosphere-only simulations that do not include coupling to the ocean (Li et al., 2018). The combined precipitation response to BC and sulfate is nearly a linear superposition of the individual responses, as can be seen by comparing Figures 1b, 1c, and 1e, and also shown explicitly in Figure S5. Linear superposition holds when perturbing BC, OC, and sulfate together (Figure 1f) and results in a similar precipitation response as BC and sulfate together (Figure 1e) due to the insignificant impact of OC on precipitation. Global and regional radiative forcing are also approximately linear (Table 1 and panel titles of Figures S3 and S4). Both aerosol direct and indirect effects contribute to these precipitation changes, and we show in Figure S6 that cloud liquid water path is significant increased due to aerosol increases.

4. Mechanisms of Monsoon Precipitation Response

Figure 2 shows the summer monsoon 850 hPa wind response (color shading for wind speed magnitude and arrows for direction) for each of our six anthropogenic forcing cases. For GHG (Figure 2a), summertime winds are enhanced over the Arabian Sea and reduced further south over the Indian Ocean and Bay of Bengal. Both of these act to invigorate the moisture-laden monsoon circulation from the southwest, delivering additional rainfall. GHGs exert an anomalous meridional temperature gradient (Figure S7) of up to 1 K due to the differential heating of the two hemispheres, which may also contribute to enhanced precipitation

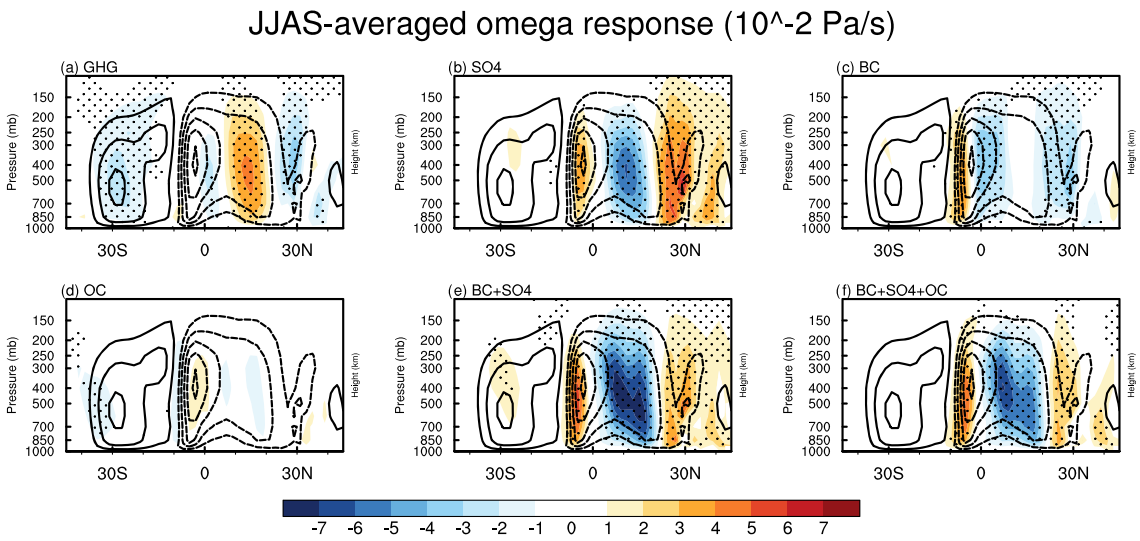

Figure 3. JJAS mean omega change in response to 2000 anthropogenic emissions compared to 1850 anthropogenic emissions for (a) greenhouse gases, (b) sulfate, (c) black carbon, (d) organic carbon aerosol, (e) black carbon and sulfate combined, and (f) black carbon, sulfate, and organic carbon aerosol combined. Stippling indicates statistical significance at the 95% confidence interval using a Student's *t* test.

in response to GHGs. Since SSTs are not changing, this temperature gradient is likely due to the larger amount of landmass in the northern versus southern hemispheres. Sulfate aerosol (Figure 2b) weakens wind speed over central India and directs it westward, leading to drying over central India. Sulfate aerosols also exert an anomalous meridional temperature gradient (magnitude of about 1 K), which may be related to the existence of a dipole pattern with wetting just south of the drying in Central India. In contrast, BC forcing strongly increase southwesterly-to-westerly moisture-laden winds resulting in enhancement of precipitation throughout most of the South Asian land mass. BC exerts a weak temperature gradient less than about 0.3 K with warming north of the equator.

As with precipitation response, horizontal winds do not strongly respond to OC, likely due to the weak impact of OC on radiative forcing in the GFDL-AM3 model caused by the lower hygroscopicity compared to sulfate. Finally, BC and sulfate together (Figure 2e) and BC, OC, and sulfate together (Figure 2f) exhibit mixtures of each of the individual wind responses, with the anomalous southwesterly-to-westerly wind response to BC forcing dominating over the Arabian Sea and Bay of Bengal.

Figure 3 shows the vertical velocity summertime response (ω) averaged over the Southeast Asian domain (50°E to 180°E longitude) in each of our anthropogenic forcing scenarios. The climatological vertical motion is shown in black contours with solid lines representing positive velocity (sinking) and dashed lines representing negative (rising). The reduced climatological rising at about 15 °N latitude due to GHG forcing (Figure 3a) explains the decrease in precipitation modeled over the Bay of Bengal, the Southeast Asia land surface, and into the South China Sea. Conversely, rising is slightly enhanced closer to 25–30°N latitude, consistent with the small increases in precipitation over most of northern India. Vertical motion is more substantially perturbed by aerosol forcing, in particular sulfate (Figure 3b). The significant decreases in precipitation over the Asian land surface, including northern India and most of China, can be explained by significant weakening of the climatological rising from 20–30°N seen in the vertical velocity data (Figure 3b). Conversely, the climatological rising is enhanced from 10–15°N which explains the corresponding precipitation increase in that latitude band that includes the Arabian Sea, Bay of Bengal, and the South China Sea. Unlike sulfate, BC significantly enhances the rising motion (Figure 3c) throughout the region north of the equator and south of 30°N, leading to the precipitation increases. Below the equator, BC forcing hinders the bottom flank of the climatological rising, corresponding to the small precipitation decreases in Figure 1c at about 5–10°S. With BC and sulfate perturbed together, the climatological rising is further enhanced compared to sulfate and BC alone. The dipole structure is also more pronounced in the sulfate and BC combined perturbation. The response of vertical velocity to OC is similar in sign to sulfate but is not statistically significant. The alternating sinking/rising motion induced by several individual climate

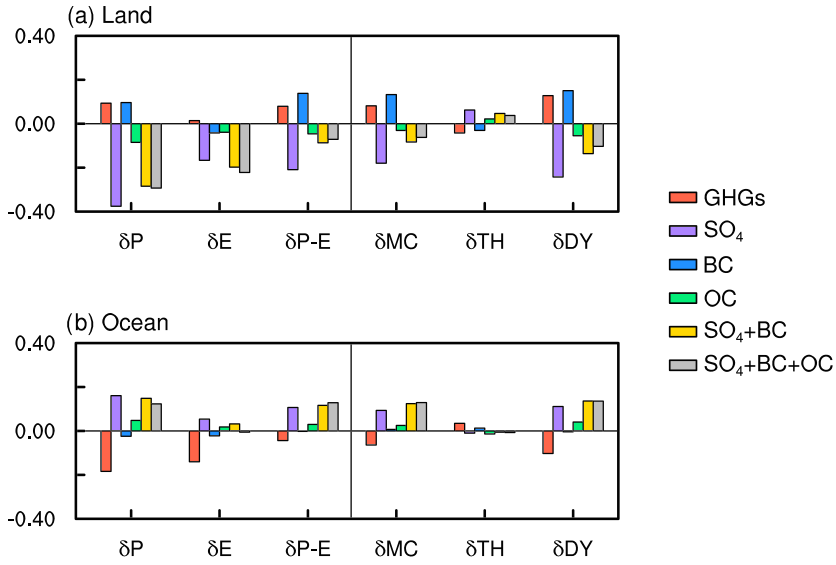

Figure 4. Land versus ocean moisture budget component change from 1850 to 2000 due to increase in anthropogenic emissions.

forcers in Figure 3 explains the dipole patterns between drying and wetting in the precipitation response (Figure 1).

5. Moisture Budget Analysis

Figure 4 shows the regional land and ocean mean precipitation, evaporation, mean column-integrated MC, and the contribution of dynamics (atmospheric circulation, DY) and thermodynamics (moisture amount, TH) to the precipitation responses to each forcing. The averaging domain is 0–50°N and 50–180°E. As reported in Figure 1, precipitation decreases in response to increased sulfate, OC, but increases in response to BC. By total precipitation rate, sulfate is the dominant driver; however, if normalized by radiative forcing, BC wields the largest influence on precipitation. When perturbed together, precipitation decreases are less than with sulfate alone due to offsetting effects of BC. Precipitation increases in response to GHG over land, though the change is relatively small compared to sulfate. Over the ocean, the signs are flipped such that precipitation increases in response to sulfate due to the side-by-side anomalous sinking and rising dipole patterns.

The change in MC is well balanced by the change in DY and TH, with the changes in DY dominant, consistent with the circulation arguments made in section 4. TH contributes very little to the overall moisture budget changes. The spatial distributions of DY and TH are shown in Figures S8 and S9. Over land, dynamic effects tend to drive decreases in MC for the scattering aerosols and increases in MC for GHG and BC. The opposite is true for TH effects, which offset a small amount of the change induced by DY effects. Over the ocean, dynamic effects contribute to increases in the moisture budget for scattering aerosols and decreases for BC and GHG, further evidence of the dipole pattern of anomalous rising and sinking. Over the ocean, the TH component is close to zero for nearly all anthropogenic forcing, since SSTs are held fixed. Evaporation contributes a substantial fraction to the P-E balance, especially over land, in response to the change in precipitation. As expected, transient eddy MC (difference between total MC and P-E) is insignificant. MC is also well balanced by the net surface water budget, P-E. Besides precipitation, additional components of the moisture budget such as DY, TH, MC, and E also appear to form linear superpositions of the individual aerosol components when those components are perturbed simultaneously.

6. Summary and Conclusions

We employ a widely used atmosphere general circulation model GFDL-AM3 to simulate the response of the South Asian summer monsoon to individual anthropogenic forcing agents including GHG, sulfate, OC, and

BC, and combinations thereof. We consider both direct and indirect aerosol effects on precipitation. Per unit radiative forcing, BC is the most effective driver of precipitation change during the South Asian summer monsoon. Sulfate is the largest driver without normalization, and relative importance of OC is small in both cases due to limited hygroscopicity. However, OC abundances are likely underestimated in climate models (Shrivastava et al., 2017). Anthropogenic GHG is an important but smaller driver than both BC and sulfate on both a normalized and non-normalized basis. When combinations of BC, sulfate, and OC are simultaneously perturbed, we find that the sulfate and BC responses dominate but the overall response is approximately a linear superposition of the individual responses.

Changes in precipitation can be mostly explained by horizontal and vertical circulation arguments. Moisture-laden flow from the Arabian Sea is invigorated by GHG and BC forcing and largely hindered by scattering aerosol forcing. In response to sulfate aerosol, the model simulates dipole patterns of drying to the north over land and wetting to the south over the ocean, which is consistent with an anomalous sinking to the north and an anomalous rising to the south over the ocean. The dynamic contribution (atmospheric circulation) to the moisture budget is responsible for the vast majority of the total precipitation response, whereas thermodynamic influences (moisture supply) are small. These changes can be caused by both direct and indirect effects of aerosols, though Li et al. (2018) found that circulation and thermodynamic changes induced by the indirect effect dominate the total response.

A caveat to this study is the use of a single atmospheric general circulation model, GFDL-AM3. However, GFDL-AM3 has been widely used for South Asian summer monsoon studies (Bollasina et al., 2011, 2013; Li et al., 2020) and simulates the monsoon with accuracy (Li & Ting, 2017). We also used a fixed SST approach which limits our results to only the fast response and not changes in SST, which are covered in Li et al. (2020). When slow responses are included as in the coupled ocean–atmosphere model, the thermodynamic contribution may be stronger, particularly for GHG forcing (Li et al., 2018). Future work should be carried out with fully coupled higher resolution CMIP6-era models.

Acknowledgments
We acknowledge a National Science Foundation AGS award number 1607348. The authors declare no conflict of interests. Data from this manuscript are publicly available here (Westervelt, 2020). The GFDL-AM3 model code is available here (https://www.gfdl.noaa.gov/am3/).

References

Albrecht (1989). Aerosols, cloud microphysics, and fractional cloudiness. *Science*, *245*(4923), 1227–1230. https://doi.org/10.1126/science.245.4923.1227

Allen, M. R., & Ingram, W. J. (2002). Constraints on future changes in climate and the hydrologic cycle. *Nature*, *419*(6903), 228–232. https://doi.org/10.1038/nature01092

Allen, R. J., Amiri-Farahani, A., Lamarque, J.-F., Smith, C., Shindell, D., Hassan, T., & Chung, C. E. (2019). Observationally constrained aerosol–cloud semi-direct effects. *Npj Climate and Atmospheric Science*, *2*, 16. https://doi.org/10.1038/s41612-019-0073-9

Biasutti, M., & Giannini, A. (2006). Robust Sahel drying in response to late 20th century forcings. *Geophysical Research Letters*, *33*, L11706. https://doi.org/10.1029/2006GL026067

Bollasina, M. A., Ming, Y., & Ramaswamy, V. (2011). Anthropogenic aerosols and the weakening of the South Asian summer monsoon. *Science*, *334*(6055), 502–505. https://doi.org/10.1126/science.1204994

Bollasina, M. A., Ming, Y., & Ramaswamy, V. (2013). Earlier onset of the Indian monsoon in the late twentieth century: The role of anthropogenic aerosols. *Geophysical Research Letters*, *40*, 3715–3720. https://doi.org/10.1002/grl.50719

Brooks, J., Allan, J. D., Williams, P. I., Liu, D., Fox, C., Haywood, J., et al. (2019). Vertical and horizontal distribution of submicron aerosol chemical composition and physical characteristics across northern India during pre-monsoon and monsoon seasons. *Atmospheric Chemistry and Physics*, *19*(8), 5615–5634. https://doi.org/10.5194/acp-19-5615-2019

Chung, E.-S., & Soden, B. J. (2017). Hemispheric climate shifts driven by anthropogenic aerosol–cloud interactions. *Nature Geoscience*, *10*(8), 566–571. https://doi.org/10.1038/NGEO2988

Donner, L. J., Wyman, B. L., Hemler, R. S., Horowitz, L. W., Ming, Y., Zhao, M., et al. (2011). The dynamical core, physical parameterizations, and basic simulation characteristics of the atmospheric component AM3 of the GFDL Global Coupled Model CM3. *Journal of Climate*, *24*(13), 3484–3519. https://doi.org/10.1175/2011JCLI3955.1

Gani, S., Bhandari, S., Seraj, S., Wang, D. S., Patel, K., Soni, P., et al. (2019). Submicron aerosol composition in the world's most polluted megacity: The Delhi aerosol supersite study. *Atmospheric Chemistry and Physics*, *19*(10), 6843–6859. https://doi.org/10.5194/acp-19-6843-2019

Garrett, T. J., & Zhao, C. (2006). Increased Arctic cloud longwave emissivity associated with pollution from mid-latitudes. *Nature*, *440*(7085), 787–789. https://doi.org/10.1038/nature04636

Gautam, R., Hsu, N. C., Lau, K.-M., & Kafatos, M. (2009). Aerosol and rainfall variability over the Indian monsoon region: Distributions, trends and coupling. *Annales Geophysicae*, *27*(9), 3691–3703. https://doi.org/10.5194/angeo-27-3691-2009

Goswami, B. N., Venugopal, V., Sangupta, D., Madhusoodanan, M. S., & Xavier, P. K. (2006). Increasing trend of extreme rain events over India in a warming environment. *Science*, *314*(5804), 1442–1445. https://doi.org/10.1126/science.1132027

Guo, L., Turner, A. G., & Highwood, E. J. (2015). Impacts of 20th century aerosol emissions on the South Asian monsoon in the CMIP5 models. *Atmospheric Chemistry and Physics*, *15*(11), 6367–6378. https://doi.org/10.5194/acp-15-6367-2015

Held, I. M., & Soden, B. J. (2006). Robust responses of the hydrological cycle to global warming. *Journal of Climate*, *19*(21), 5686–5699. https://doi.org/10.1175/JCLI3990.1

Jimenez, J. L., Canagaratna, M. R., Donahue, N. M., Prevot, A. S. H., Zhang, Q., Kroll, J. H., et al. (2009). Evolution of organic aerosols in the atmosphere. *Science (New York, N.Y.)*, *326*(5959), 1525–1529. https://doi.org/10.1126/science.1180353

Lamarque, J.-F., Bond, T. C., Eyring, V., Granier, C., Heil, A., Klimont, Z., et al. (2010). Historical (1850–2000) gridded anthropogenic and biomass burning emissions of reactive gases and aerosols: Methodology and application. *Atmospheric Chemistry and Physics*, *10*(15), 7017–7039. https://doi.org/10.5194/acp-10-7017-2010

Lau, K.-M., & Kim, K.-M. (2006). Observational relationships between aerosol and Asian monsoon rainfall, and circulation. *Geophysical Research Letters*, *33*, L21810. https://doi.org/10.1029/2006GL027546

Lau, W. K. M., & Kim, K. M. (2017). Competing influences of greenhouse warming and aerosols on Asian summer monsoon circulation and rainfall. *Asia-Pacific Journal of Atmospheric Sciences*, *53*(2), 181–194. https://doi.org/10.1007/s13143-017-0033-4

Li, X., & Ting, M. (2017). Understanding the Asian summer monsoon response to greenhouse warming: The relative roles of direct radiative forcing and sea surface temperature change. *Climate Dynamics*, *49*(7–8), 2863–2880. https://doi.org/10.1007/s00382-016-3470-3

Li, X., Ting, M., & Lee, D. E. (2018). Fast adjustments of the Asian summer monsoon to anthropogenic aerosols. *Geophysical Research Letters*, *45*, 1001–1010. https://doi.org/10.1002/2017GL076667

Li, X., Ting, M., Li, C., & Henderson, N. (2015). Mechanisms of Asian summer monsoon changes in response to anthropogenic forcing in CMIP5 models*. *Journal of Climate*, *28*(10), 4107–4125. https://doi.org/10.1175/JCLI-D-14-00559.1

Li, X., Ting, M., You, Y., Lee, D., Westervelt, D. M., & Ming, Y. (2020). South Asian summer monsoon response to aerosol-forced sea surface temperatures. *Geophysical Research Letters*, *47*, e2019GL085329. https://doi.org/10.1029/2019GL085329

Li, Z., Lau, W. K. M., Ramanathan, V., Wu, G., Ding, Y., Manoj, M. G., et al. (2016). Aerosol and monsoon climate interactions over Asia. *Reviews of Geophysics*, *54*, 866–929. https://doi.org/10.1002/2015RG000500

Li, Z., Wang, Y., Guo, J., Zhao, C., Cribb, M. C., Dong, X., et al. (2019). East Asian study of tropospheric aerosols and their impact on regional clouds, precipitation, and climate (EAST-AIRCPC). *Journal of Geophysical Research: Atmospheres*, *124*(23), 13,026–13,054. https://doi.org/10.1029/2019JD030758

Liepert, B. G., & Previdi, M. (2009). Do models and observations disagree on the rainfall response to global warming? *Journal of Climate*, *22*(11), 3156–3166. https://doi.org/10.1175/2008JCLI2472.1

Liu, L., Shawki, D., Voulgarakis, A., Kasoar, M., Samset, B. H., Myhre, G., et al. (2018). A PDRMIP multimodel study on the impacts of regional aerosol forcings on global and regional precipitation. *Journal of Climate*, *31*(11), 4429–4447. https://doi.org/10.1175/JCLI-D-17-0439.1

Marvel, K., & Bonfils, C. (2013). Identifying external influences on global precipitation. *Proceedings of the National Academy of Sciences of the United States of America*, *110*(48), 19,301–19,306. https://doi.org/10.1073/pnas.1314382110

Meehl, G. A., Arblaster, J. M., Collins, W. D., Meehl, G. A., Arblaster, J. M., & Collins, W. D. (2008). Effects of black carbon aerosols on the Indian monsoon. *Journal of Climate*, *21*(12), 2869–2882. https://doi.org/10.1175/2007JCLI1777.1

Meinshausen, M., Smith, S. J., Calvin, K., Daniel, J. S., Kainuma, M. L. T., Lamarque, J.-F., et al. (2011). The RCP greenhouse gas concentrations and their extensions from 1765 to 2300. *Climatic Change*, *109*(1–2), 213–241. https://doi.org/10.1007/s10584-011-0156-z

Menon, S., Hansen, J., Nazarenko, L., & Luo, Y. (2002). Climate effects of black carbon aerosols in China and India. *Science*, *297*(5590), 2250–2253. https://doi.org/10.1126/science.1075159

Ming, Y., Ramaswamy, V., Donner, L. J., & Phillips, V. T. J. (2006). A new parameterization of cloud droplet activation applicable to general circulation models. *Journal of the Atmospheric Sciences*, *63*(4), 1348–1356. https://doi.org/10.1175/JAS3686.1

Ming, Y., Ramaswamy, V., & Persad, G. (2010). Two opposing effects of absorbing aerosols on global-mean precipitation. *Geophysical Research Letters*, *37*, L13701. https://doi.org/10.1029/2010GL042895

Naik, V., Horowitz, L. W., Fiore, A. M., Ginoux, P., Mao, J., Aghedo, A. M., & Levy, H. (2013). Impact of preindustrial to present-day changes in short-lived pollutant emissions on atmospheric composition and climate forcing. *Journal of Geophysical Research: Atmospheres*, *118*, 8086–8110. https://doi.org/10.1002/jgrd.50608

Penner, J. E., Quaas, J., Storelvmo, T., Takemura, T., Boucher, O., Guo, H., et al. (2006). Model intercomparison of indirect aerosol effects. *Atmospheric Chemistry and Physics*, *6*(11), 3391–3405. https://doi.org/10.5194/acp-6-3391-2006

Petters, M. D., & Kreidenweis, S. M. (2007). A single parameter representation of hygroscopic growth and cloud condensation nucleus activity. *Atmospheric Chemistry and Physics*, *7*(8), 1961–1971. https://doi.org/10.5194/acp-7-1961-2007

Pfahl, S., O'Gorman, P. A., & Fischer, E. M. (2017). Understanding the regional pattern of projected future changes in extreme precipitation. *Nature Climate Change*, *7*(6), 423–427. https://doi.org/10.1038/nclimate3287

Ramanathan, V., Crutzen, P. J., Kiehl, J. T., & Rosenfeld, D. (2001). Aerosols, climate, and the hydrological cycle. *Science (New York, N.Y.)*, *294*(5549), 2119–2124. https://doi.org/10.1126/science.1064034

Ramanathan, V., Li, F., Ramana, M. V., Praveen, P. S., Kim, D., Corrigan, C. E., et al. (2007). Atmospheric brown clouds: Hemispherical and regional variations in long-range transport, absorption, and radiative forcing. *Journal of Geophysical Research*, *112*, D22S21. https://doi.org/10.1029/2006JD008124

Rosenfeld, D., Lohmann, U., Raga, G. B., O'Dowd, C. D., Kulmala, M., Fuzzi, S., et al. (2008). Flood or drought: How do aerosols affect precipitation? *Science (New York, N.Y.)*, *321*(5894), 1309–1313. https://doi.org/10.1126/science.1160606

Samset, B. H., Myhre, G., Forster, P. M., Hodnebrog, Ø., Andrews, T., Faluvegi, G., et al. (2016). Fast and slow precipitation responses to individual climate forcers: A PDRMIP multimodel study. *Geophysical Research Letters*, *43*, 2782–2791. https://doi.org/10.1002/2016GL068064

Sanap, S. D., & Pandithurai, G. (2015). The effect of absorbing aerosols on Indian monsoon circulation and rainfall: A review. *Atmospheric Research*. Elsevier Ltd, *164-165*, 318–327. https://doi.org/10.1016/j.atmosres.2015.06.002

Schnell, J. L., Naik, V., Horowitz, L. W., Paulot, F., Mao, J., Ginoux, P., et al. (2018). Exploring the relationship between surface $PM_{2.5}$ and meteorology in Northern India. *Atmospheric Chemistry and Physics*, *18*(14), 10,157–10,175. https://doi.org/10.5194/acp-18-10157-2018

Seager, R., & Henderson, N. (2013). Diagnostic computation of moisture budgets in the ERA-Interim reanalysis with reference to analysis of CMIP-archived atmospheric model data. *Journal of Climate*, *26*(20), 7876–7901. https://doi.org/10.1175/JCLI-D-13-00018.1

Seager, R., Neelin, D., Simpson, I., Liu, H., Henderson, N., Shaw, T., et al. (2014). Dynamical and thermodynamical causes of large-scale changes in the hydrological cycle over North America in response to global warming. *Journal of Climate*, *27*(20), 7921–7948. https://doi.org/10.1175/JCLI-D-14-00153.1

Shen, L., & Zhao, C. (2020). Dominance of shortwave radiative heating in the sea-land breeze amplitude and its impacts on atmospheric visibility in Tokyo, Japan. *Journal of Geophysical Research: Atmospheres*, *125*, e2019JD031541. https://doi.org/10.1029/2019JD031541

Shrivastava, M., Cappa, C. D., Fan, J., Goldstein, A. H., Guenther, A. B., Jimenez, J. L., et al. (2017). Recent advances in understanding secondary organic aerosol: Implications for global climate forcing. *Reviews of Geophysics*, *55*, 509–559. https://doi.org/10.1002/2016RG000540

Singh, D. (2016). South Asian monsoon: Tug of war on rainfall changes. *Nature Climate Change*. Nature Publishing Group, *6*(1), 20–22. https://doi.org/10.1038/nclimate2901

Stevens, B., & Feingold, G. (2009). Untangling aerosol effects on clouds and precipitation in a buffered system. *Nature*, *461*(7264), 607–613. https://doi.org/10.1038/nature08281

Turner, A. G., & Annamalai, H. (2012). Climate change and the South Asian summer monsoon. *Nature Climate Change*. Nature Publishing Group, *2*(8), 587–595. https://doi.org/10.1038/nclimate1495

Twomey, S. A. (1977). Pollution and cloud albedo. *Eos Transactions American Geophysical Union*, *58*(8), 797–797.

Undorf, S., Polson, D., Bollasina, M. A., Ming, Y., Schurer, A., & Hegerl, G. C. (2018). Detectable impact of local and remote anthropogenic aerosols on the 20th century changes of West African and South Asian monsoon precipitation. *Journal of Geophysical Research: Atmospheres*, *123*, 4871–4889. https://doi.org/10.1029/2017JD027711

Wang, H., Xie, S.-P., & Liu, Q. (2016). Comparison of climate response to anthropogenic aerosol versus greenhouse gas forcing: Distinct patterns. *Journal of Climate*, *29*(14), 5175–5188. https://doi.org/10.1175/JCLI-D-16-0106.1

Webster, P. J., Magaña, V. O., Palmer, T. N., Shukla, J., Tomas, R. A., Yanai, M., & Yasunari, T. (1998). Monsoons: Processes, predictability, and the prospects for prediction. *Journal of Geophysical Research*, *103*(C7), 14,451–14,510. https://doi.org/10.1029/97JC02719

Westervelt, D. M., Conley, A. J., Fiore, A. M., Lamarque, J.-F., Shindell, D., Previdi, M., et al. (2017). Multimodel precipitation responses to removal of U.S. sulfur dioxide emissions. *Journal of Geophysical Research: Atmospheres*, *122*, 5024–5038. https://doi.org/10.1002/2017JD026756

Westervelt, Dan (2020). Asian summer monsoon. [figshare. Dataset.] https://doi.org/10.6084/m9.figshare.12043062.v1

Westervelt, D. M., Conley, A. J., Fiore, A. M., Lamarque, J.-F., Shindell, D. T., Previdi, M., et al. (2018). Connecting regional aerosol emissions reductions to local and remote precipitation responses. *Atmospheric Chemistry and Physics*, *18*(16), 12,461–12,475. https://doi.org/10.5194/acp-18-12461-2018

Westervelt, D. M., Mascioli, N. R., Fiore, A. M., Conley, A. J., Lamarque, J.-F., Shindell, D. T., et al. (2020). Local and remote mean and extreme temperature response to regional aerosol emissions reductions. *Atmospheric Chemistry and Physics*, *20*(5), 3009–3027. https://doi.org/10.5194/acp-20-3009-2020

Wilcox, L., Liu, Z., Samset, B., Hawkins, E., Lund, M., Nordling, K., et al. (2020). Accelerated increases in global and Asian summer monsoon precipitation from future aerosol reductions. *Atmospheric Chemistry and Physics Discussions*. https://doi.org/10.5194/acp-2019-1188

Zhao, C., Yang, Y., Fan, H., Huang, J., Fu, Y., Zhang, X., et al. (2019). Aerosol characteristics and impacts on weather and climate over the Tibetan Plateau. *National Science Review*, *7*(3), 492–495. https://doi.org/10.1093/nsr/nwz184